On-Demand Dark Soliton Train Manipulation in a Spinor Polariton Condensate

F. Pinsker[1,*] and H. Flayac[2,†]
[1]Department of Applied Mathematics and Theoretical Physics, University of Cambridge, Wilberforce Road, Cambridge CB3 0WA, United Kingdom
[2]Institute of Theoretical Physics, École Polytechnique Fédérale de Lausanne EPFL, CH-1015 Lausanne, Switzerland
(Received 31 October 2013; published 10 April 2014)

We theoretically demonstrate the generation of dark soliton trains in a one-dimensional exciton-polariton condensate within experimentally accessible schemes. In particular, we show that the frequency of the train can be finely tuned fully optically or electrically to provide a stable and efficient output signal modulation. Taking the polarization of the condensate into account, we elucidate the possibility of forming on-demand half-soliton trains.

DOI: 10.1103/PhysRevLett.112.140405 PACS numbers: 03.75.Kk, 03.65.-w, 05.45.-a, 67.85.Hj

Introduction.—The first unambiguous observation of Bose-Einstein condensation in dilute Bose gases at low temperature [1] set off an avalanche of research on this new state of matter. The lowest energy fraction of a degenerated Bose gas occupying low energy modes obeys the property of vanishing viscosity and does not take part in the dissipation of momentum, a phenomenon referred to as superfluidity [2]. This holds true as long as the condensate is only slightly disturbed [3]. As soon as strong dynamical density modulations occur, e.g., when the condensate is abruptly brought out of its equilibrium through an external perturbation, it responds in a unique way by generating robust elementary excitations such as solitons or vortices [4].

More recently the concept of macroscopically populated single particle states [5,6] was transposed to a variety of mesoscopic systems such as cavity photons [7,8], magnons [9], indirect excitons [10], exciton-polaritons (polaritons) [11], and even classical waves [12]. In the proper regime, all of those systems can be described by complex-valued order parameters—the condensate wave functions—with dynamics governed by nonlinear Schrödinger-type equations such as the Gross-Pitaevskii [13] and the complex Ginzburg-Landau equation [14]. Here the nonlinearity associated with self-interactions plays an essential role in the possible states with or without excitations, their dynamics, and, in particular, their stability [15]. Similarly, in the slowly varying envelope approximation, light waves can be approximated by complex-valued wave functions governed by nonlinear Schrödinger-type equations that are formally comparable to those of Bose-Einstein condensates and thus show analog dynamical behavior such as stationary and moving optical dark or bright solitons in quasi-1D settings [16,17].

For several decades light waves have been utilized in a wide range of applications such as in nonlinear fiber optic communication [16,18–20] while research on new technologies is thriving, in particular, on elementary circuit components such as optical diodes [21], transistors [22], or realizations of analog devices involving exciton-polariton condensates [23,24] and conceptually on optical computing schemes [25].

Exciton-polaritons are half-light half-matter quasiparticles formed in semiconductor microcavities and allow high-speed propagation from their photonic part while having strong self-interaction from their excitonic fraction. They are extremely promising from both fundamental and technological points of view given the ease it provides to finely control the parameters of their condensate now routinely produced in different geometries (see, e.g., Ref. [26]). Indeed, state-of-the-art technology allows us to etch any sample shape to sculpt the confining potential seen by the condensate at will. It explains the plethora of recent proposals [27–34] for polariton devices, some of which have been experimentally implemented [23,24,35]. The main advantage with respect to standard optical systems in nonlinear media is the very large exciton-mediated nonlinear response of the system reducing the required input power by orders of magnitude. Recently, there was a growing interest in demonstrating the formation of (spin-polarized) topological defects [36–40] that are now envisaged as stable information carriers [41–43] within a young field of research called spin-optronics [44].

In this Letter, we present experimentally accessible schemes for the intended generation and manipulation of stable and fully controllable wave patterns within a quasi-1D microcavity. We demonstrate the on-demand formation of dark soliton trains within a quasi-1D channel and the optical and electrical dynamical control of their frequency. Finally, we demonstrate the possibility of controlling the polarization of the soliton trains.

The model.—We consider the system modeled in Fig. 1, namely a wire-shaped microcavity similar to the one implemented in Ref. [45] that bounds the polaritons to a quasi-1D channel. A metallic contact is embed over half of the sample to form a potential step seen by the polaritons and whose amplitude can be tuned on demand applying an electric field [46]. The spinor polariton field $\boldsymbol{\psi} = (\psi_+, \psi_-)^T$ evolves along a set of effectively 1D complex Ginzburg-Landau equations coupled to a rate equation for the excitonic reservoir [46,47],

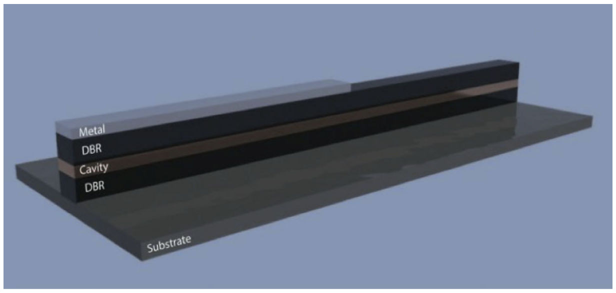

FIG. 1 (color online). Model of a potential sample consisting in a quasi-1D microcavity [distributed Bragg reflectors (DBR)] embedding a metallic deposition over half of its length to form a potential step. A gate voltage can be applied to the metal to tune dynamically the step amplitude.

$$i\hbar\frac{\partial\psi_+}{\partial t} = \left[-\frac{\hbar^2\Delta}{2m} + \alpha_1(|\psi_+|^2 + n_R) + \alpha_2|\psi_-|^2\right]\psi_+ + \left[U - \frac{i\hbar}{2}(\Gamma - \gamma n_R)\right]\psi_+ - \frac{H_x}{2}\psi_-, \quad (1)$$

$$i\hbar\frac{\partial\psi_-}{\partial t} = \left[-\frac{\hbar^2\Delta}{2m} + \alpha_1(|\psi_-|^2 + n_R) + \alpha_2|\psi_+|^2\right]\psi_- + \left[U - \frac{i\hbar}{2}(\Gamma - \gamma n_R)\right]\psi_- - \frac{H_x}{2}\psi_+, \quad (2)$$

$$\frac{\partial n_R}{\partial t} = P - \Gamma_R n_R - \gamma(|\psi_+|^2 + |\psi_-|^2)n_R. \quad (3)$$

This model describes in a simple way the phenomenology of the condensate formation under nonresonant pumping. We assume a parabolic dispersion of polaritons associated with an effective mass $m = 5\times10^{-5}m_0$, where m_0 is that of the free electron and a decay rate $\Gamma = 1/100\ \mathrm{ps}^{-1}$. $U(x,t) = [U(t) + U_0]H(x)$, where $H(x)$ is the Heaviside function, $U_0 = -0.5$ meV is the step height induced by the presence of the metal solely, and $U(t)$ is the potential landscape imposed by the external electric field. $\alpha_1 = 6xE_b a_B^2/S = 1.2\times10^{-3}\ \mathrm{meV}\cdot\mu\mathrm{m}$ and $\alpha_2 = -0.1\alpha_1$ are, respectively, the parallel and antiparallel spin interaction strength given that x, E_b, and a_B are the excitonic fraction, binding energy, and Bohr radius, respectively, and S is the pump spot area. $H_x = 0.01$ meV is the strength of the effective magnetic field induced by the energy splitting between TE and TM eigenmodes that couples the spin components [35]. The excitonic reservoir characterized by the decay rate $\Gamma_R = 1/400\ \mathrm{ps}^{-1}$ is driven by the pump term $P = A_P\exp(-x^2/\sigma^2)$, where $\sigma = 20\,\mu$m and A_P is taken in the range of hundreds of Γ_R. It exchanges particles with the polariton condensate at a rate $\gamma = 2\times10^{-2}\Gamma_R$.

We note that, while the stimulated scattering is taken into account by Eqs. (1)–(3), energy relaxation processes dominant under the pump spot, apart from the lifetime induced decay of the interactions energy, are neglected in this framework and could be treated, e.g., within the formalisms of Refs. [48,49]. Energy relaxation would not impact our results qualitatively especially for the finite pump spot size we consider here.

Soliton train generation.—As shown in Ref. [4], a local abrupt change of self-interaction strength of the condensate leads to the formation of a stable and regular dark soliton train. When the flow in the direction of decreasing interaction due to particle repulsions is locally crossing the speed of sound $c_s(x) = \sqrt{\mu(x)/m}$, where $\mu(x) = \alpha_1 n(x)$ (for a scalar condensate) at the point of abrupt change in self-interactions, solitons are formed from dispersive shock waves [50] that dissipate the local excess of energy. In polariton condensates the interaction strength α_1 is varied tuning the exciton or photon detuning and therefore the excitonic fraction, but it can hardly be made inhomogeneous within a given sample nor tuned dynamically. A valuable alternative we follow here is to introduce the tunable potential step $U(x,t)$ in Eqs. (1) and (2). The mechanism for soliton generation is the following (see Ref. [51] for a more details). Let us suppose we have a homogeneous density n_0 at $t = 0$ and neglect the finite lifetime and pumping of quasiparticles and the geometry of our pump spot. Then, taking the potential U stepwise for all following $t > 0$, we get close to the breaking point at $x = 0$, the density n_1 for $x = 0^-$ and n_2 as $x = 0^+$, and we say $n_1 = kn_2$, with $1 > k > 0$. Using momentum and mass conservation at $x = 0$, we find the simple criterion $0.6404 > k$ to break the speed of sound in the region $x < 0$, which is in good agreement with our numerical results. In the regime of soliton-train generation, the train frequency ν increases with the magnitude of the potential step [51] as the corresponding increase of mass passing the step at $x = 0$ allows a more frequent breaking of the local speed of sound. This is analogous to the situation of a superfluid passing an obstacle above criticality for which greater mass transport is equivalent to a higher number of generated vortices in 2D [52].

For a given metal type and deposition thickness on top of the microcavity, Tamm plasmon-polariton modes [53] were predicted to form at the interface inducing a local redshift of the polariton resonances of amplitude U_0 and the required potential step. We note that in the absence of plasmon, the interface would form a Schottky junction known to blue detune the polariton modes [54]. The application of a voltage to the metal produces the additional gate redshift $U(t)$ through the excitonic Stark effect up to a few meVs for voltages lying in the range of tens of kV/cm [55] and standing for the input modulation of the polariton condensate. The nonresonant excitation of the system is crucial since in this context the condensate phase is free to evolve under the pump spot in contrast to a resonant injection scheme that would imprint the phase preventing the onset of solitons.

Optical control.—Let us start with the simplest passive configuration where no voltage is applied and therefore the potential step is *fixed*. We switch on the pump laser focused on the step at $t = 0$ and wait for the steady state to be reached. The reservoir is filled by the incoherent pump and the stimulation towards the lowest polariton energy state

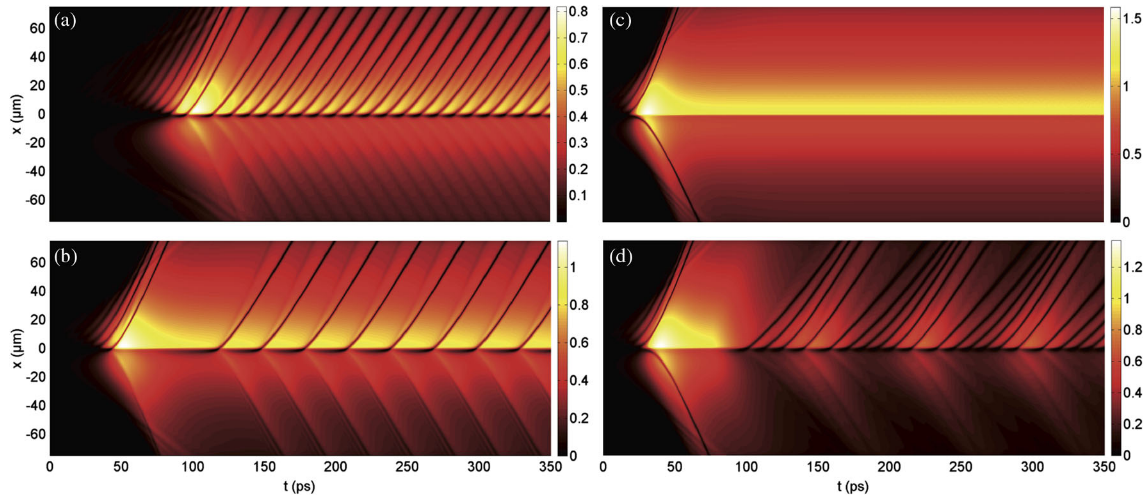

FIG. 2 (color online). Optical control. (a)–(c) Results obtained by pumping over the potential step with increasing pump amplitude of $200\Gamma_R$, $375\Gamma_R$, and $600\Gamma_R$, respectively. Here, we monitor $\mu(x,t)$ (meV) in the color map. (d) Sinusoidal modulation of the pump amplitude between 0 and $500\Gamma_R$ and with a period $T = 100$ ps resulting in signal frequency modulation.

occurs, forming the condensate with a chemical potential $\mu = (\alpha_1 + \alpha_2)n/2 - H_x/2$ (corresponding to the measurable blueshift of the polariton emission), where $n = |\psi_+|^2 + |\psi_-|^2 = n_+ + n_-$ is the total polariton density. Given the interrelation $\alpha_1 > \alpha_2$, the condensate interaction energy is minimized for a linear polarization, meaning that $n_+ = n_-$, and the condensate is said to be antiferromagnetic [56]. The linear polarization orientation is homogeneous at zero temperature and fixed by the H_x contribution, namely, along the axis of the wire. In our model we trigger the condensation on the x-polarized ground state with weak initial populations $n_\pm^0$. Figure 2 shows numerical solutions to Eqs. (1)–(3). We depict the chemical potential $\mu(x,t)$ for crescent pump amplitudes A_P. We clearly see the decrease in the train frequency ν with increasing pump power [Figs. 2(a) and 2(b)] until the train vanishes [Fig. 2(c)].

The condensate heals from the step forming an asymmetric gray soliton resulting from the local velocity gradient, as it happens, e.g., at the boundaries of a condensate trapped in a square potential. The depth of the soliton is imposed by the local background density and velocity. For a high enough background density, the flow is superfluid ($v < c_s$) both around the step and within the soliton that remains pinned to the step preventing the train onset [Fig. 2(c)]. For lower densities, the speed of sound can be surpassed at the soliton core, which allows the condensate to dissipate the local excess of energy via a dispersive shock wave [50] (see movies in the Supplemental Material [51]) that releases the soliton to the side where the background flow is the highest. Then it takes some time for the condensate to form a new soliton. The higher the density, the stiffer the condensate and, therefore, the more time it takes to form a new density depletion. This response determines the quasilinear train frequency ν dependence over the chemical potential shown in the Supplemental Material [51].

Our results demonstrate the possibility to modulate passively an optical signal via the formation of stable dark solitons varying the pump amplitude. The dark soliton signals shall then be detected experimentally at the output via one of the schemes proposed in the context of nonlinear optics [57] to encode information. Indeed, as proposed in Ref. [58], soliton trains can be used to store numbers determined uniquely by an adjustable ν. So far, most of the device proposals involving microcavity polaritons have focused on signal transmission but never on its modulation. Nonetheless, as one can see, the train frequencies lie in the range of THz allowing us to perform very high-speed processing due to the polariton photonic part combined with a large exciton-mediated nonlinear response.

In Fig. 2(d), we show an example of sinusoidal input power modulation that leads to a dynamical variation of ν or a modulation of the output on demand to produce useful wave packets. The main advantage of this all-optical input modulation scheme is that it allows us to reach high-speed variation of ν while the drawback is that the background density of the condensate is obviously affected as well. Finally, we note that this setup involving a fixed potential step does not specifically require a metallic deposition. A sample split in two parts with slightly different lateral width might be sufficient to reproduce the effects discussed above.

Electric control.—Now we consider the case where the pump power is fixed and, in addition, an electric field is applied to the metallic contact to modulate the potential step height. Under such assumptions, the chemical potential μ is globally fixed. The higher the step (the electric field), the larger the density gradient and, hence, one encounters a greater mass transport towards lower energy regions. So, similarly to Ref. [52], we obtain an increase in dark soliton train frequency, as shown in Ref. [51]. To demonstrate this behavior, in Fig. 3(a) we show the results obtained by ramping down linearly the potential step from 0 to -1.5 meV, which corresponds to an increase in the electric field amplitude. We clearly see the linear increase in ν versus time.

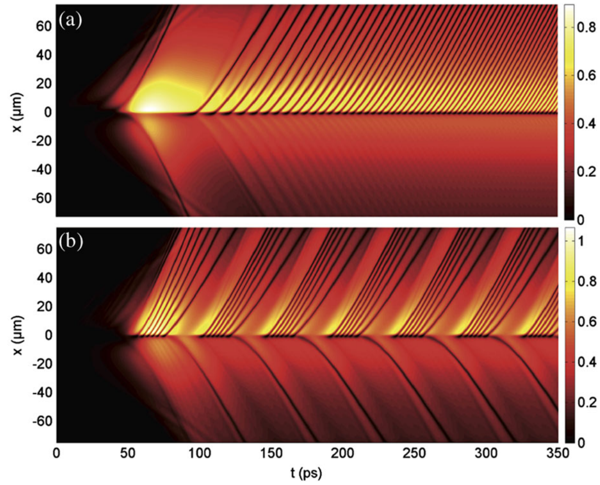

FIG. 3 (color online). Electric control of the dark soliton trains. (a) The potential step amplitude $U(t)$ is linearly ramped down versus time from 0 to -1.5 meV. (b) Sinusoidal modulation of the step between 0 and -1.5 meV with a period of 50 ps.

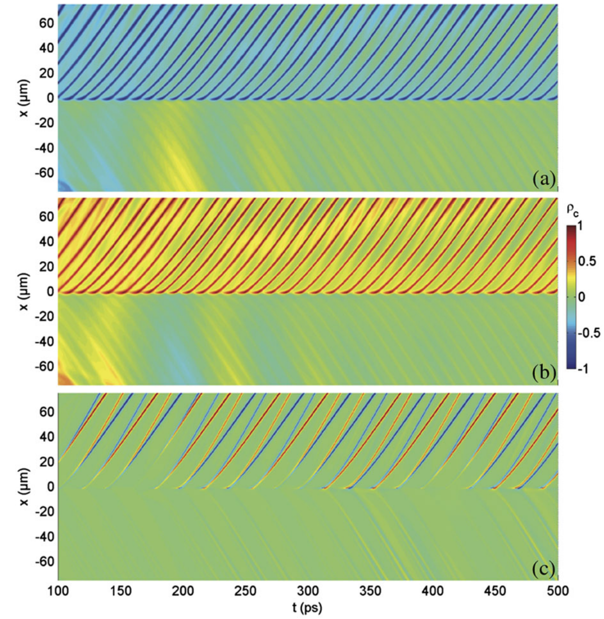

FIG. 4 (color online). Control over the polarization of the trains. The color map shows the degree of circular polarization ρ_c. (a) $\gamma_2/\gamma_1 = 0.90$, (b) $\gamma_2/\gamma_1 = 1.11$, and (c) $\gamma_2/\gamma_1 = 0.99$.

Similarly to the results of Fig. 2(d), in Fig. 3(b) we show results obtained from a sinusoidal modulation of the potential step amplitude producing an efficient dynamical modulation of the output signal in the form of wave packets. Such an electric control of the polariton flow has the advantage of impacting weakly on the background density, but there might be some technological limitation on the switching speed.

Polarization control.—So far, we have discussed a phenomenology that could be reproduced using a scalar condensate without any need for its spinor character. Indeed, we have considered the ideal case of a perfectly linearly polarized condensate with no polarization symmetry breaking, namely, $n_+(x) = n_-(x)$ for any x position. The consequence is that the dark solitons formed in one spin component are perfectly overlapping with the ones in the other component and are behaving as scalar ones. However, in real experimental situations, the fluctuations brought by the structural disorder or the background noise can affect the linear polarization of the condensate leading to local inhomogeneities slightly breaking the polarization symmetry or the equivalence between the two spin components. As discussed in Ref. [42], these fluctuations can lead to the separation of dark solitons in each component to form pairs of half-solitons [39,40]. As soon as they are split, they will repel each other under the condition $\alpha_2 < 0$ and start to feel an effective magnetic force imposed by H_x and be accelerated or slowed down depending on their linear polarization texture [42]. This effect produced by local inhomogeneities or random processes would obviously be harmful to the formation of a deterministic spin signal. However, as was observed experimentally in Ref. [59], using a polarized excitation laser can lead to the formation of a circularly or elliptically polarized condensate due to the long characteristic spin relaxation times of excitons. In Fig. 4, we show results capitalizing on this effect to produce a useful spin signal.

We have modeled a slightly elliptically polarized nonresonant pump introducing two different reservoir or condensate transfer rates γ_1 and γ_2 in Eqs. (1) and (2). We have adjusted the ratio γ_2/γ_1 to 0.90, 1.11, and 0.99 in Figs. 4(a)–4(c), respectively. The color map shows the degree of circular polarization $\rho_c(x,t) = (n_+ - n_-)/(n_+ + n_-)$ of the polariton emission. We see that the weak ensuing density imbalance between the two spin components of the condensate leads to a well-defined polarization symmetry breaking inducing either the formation of trains of pairs of half-solitons [Fig. 4(c)] or trains of half-solitons with a well-defined polarization for larger imbalances [Figs. 4(a) and 4(b)]. It means that not only the frequency of the trains can be finely tuned, but also their polarization by variation of the input polarization. It provides another degree of freedom to code information.

Conclusions.—We have shown the strong potential of microcavities for high-speed optical signal modulation and information coding. Our proposal involves the all-optical or electric control of dark soliton trains within realistic scheme. We have demonstrated the possibility to tune both the train frequency and its polarization. The present concept could not only play a central role at the heart of future high-speed polariton circuits within the rapidly expanding field of spin-optronics but also allow the very first observation of dark soliton trains in a quantum fluid.

F. P. acknowledges financial support from the UK Engineering and Physical Sciences Research Council (EPSRC) Grant No. EP/H023348/1 for the University of Cambridge Centre for Doctoral Training, the Cambridge Centre for Analysis, and a KAUST grant. H. F. acknowledges financial support from NCCR Quantum Photonics (NCCR QP), research instrument of the Swiss National

Science Foundation (SNSF). We thank F. Manni, A. Dreismann, and N. Berloff for fruitful discussions and are very grateful for the referee's remarks.

*fp278@cam.ac.uk
†hugo.flayac@epfl.ch

[1] M. H. Anderson, J. R. Ensher, M. R. Matthews, C. E. Wieman, and E. A. Cornell, Science **269**, 198 (1995).
[2] F. London, Nature (London) **141**, 643 (1938).
[3] C. Raman, M. Köhl, R. Onofrio, D. Durfee, C. Kuklewicz, Z. Hadzibabic, and W. Ketterle, Phys. Rev. Lett. **83**, 2502 (1999).
[4] F. Pinsker, N. G. Berloff, and V. M. Pérez-García, Phys. Rev. A **87**, 053624 (2013).
[5] A. Einstein, Sitzungsber. Preuss. Akad. Wiss. Phys. Math. Kl. **3**, 3 (1925).
[6] L. Onsager and O. Penrose, Phys. Rev. **104**, 576 (1956).
[7] J. Klaers, J. Schmitt, F. Vewinger, and M. Weitz, Nature (London) **468**, 545 (2010).
[8] I. Carusotto and C. Ciuti, Rev. Mod. Phys. **85**, 299 (2013).
[9] O. Demokritov, V. E. Demidov, O. Dzyapko, G. A. Melkov, A. A. Serga, B. Hillebrands, and A. N. Slavin, Nature (London) **443**, 430 (2006).
[10] L. V. Butov, J. Phys. Condens. Matter **19**, 295202 (2007).
[11] J. Kasprzak *et al.*, Nature (London) **443**, 409 (2006).
[12] C. Sun, S. Jia, C. Barsi, S. Rica, A. Picozzi, and J. W. Fleischer, Nat. Phys. **8**, 471 (2012).
[13] L. P. Pitaevskii and S. Stringari, *Bose Einstein Condensation* (Clarendon, Oxford, 2003).
[14] J. Keeling and N. G. Berloff, Phys. Rev. Lett. **100**, 250401 (2008).
[15] I. S. Aranson and L. Kramer, Rev. Mod. Phys. **74**, 99 (2002).
[16] G. P. Agrawal, *Nonlinear Science at the Dawn of the 21st Century*, Lecture Notes in Physics Vol. 542 (Springer, Berlin, Heidelberg, 2000), pp. 195–211.
[17] J. Scheuer, M. Orenstein, and D. Arbel, J. Opt. Soc. Am. B **19**, 2384 (2002).
[18] G. P. Agrawal and H. A. Haus, Phys. Today **55**, No. 6, 58 (2002).
[19] D. Woods and T. J. Naughton, Nat. Phys. **8**, 257 (2012).
[20] E. M. Dianov, P. V. Mamyshev, and A. M. Prokhorov, Sov. J. Quantum Electron. **18**, 1 (1988).
[21] L. Bi, J. Hu, P. Jiang, D. H. Kim, G. F. Dionne, L. C. Kimerling, and C. A. Ross, Nat. Photonics **5**, 758 (2011).
[22] C. Wenlan, K. M. Beck, R. Bucker, M. Gullans, M. D. Lukin, H. Tanji-Suzuki, and V. Vuletic, Science **341**, 768 (2013).
[23] D. Ballarini, M. De Giorgi, E. Cancellieri, R. Houdré, E. Giacobino, R. Cingolani, A. Bramati, G. Gigli, and D. Sanvitto, Nat. Commun. **4**, 1778 (2013).
[24] C. Antón, T. C. H. Liew, J. Cuadra, M. D. Martín, P. S. Eldridge, Z. Hatzopoulos, G. Stavrinidis, P. G. Savvidis, and L. Viña, Phys. Rev. B **88**, 245307 (2013).
[25] D. Woods and T. J. Naughton, Applied Mathematics and Computation **215**, 1417 (2009).
[26] G. Tosi, G. Christmann, N. G. Berloff, P. Tsotsis, T. Gao, Z. Hatzopoulos, P. G. Savvidis, and J. J. Baumberg, Nat. Phys. **8**, 190 (2012).
[27] T. Gao, P. S. Eldridge, T. C. H. Liew, S. I. Tsintzos, G. Stavrinidis, G. Deligeorgis, Z. Hatzopoulos, and P. G. Savvidis, Phys. Rev. B **85**, 235102 (2012).
[28] T. C. H. Liew, M. M. Glazov, K. V. Kavokin, I. A. Shelykh, M. A. Kaliteevski, and A. V. Kavokin, Phys. Rev. Lett. **110**, 047402 (2013).
[29] T. C. H. Liew, A. V. Kavokin, and I. A. Shelykh, Phys. Rev. Lett. **101**, 016402 (2008).
[30] I. A. Shelykh, G. Pavlovic, D. D. Solnyshkov, and G. Malpuech, Phys. Rev. Lett. **102**, 046407 (2009).
[31] I. A. Shelykh, R. Johne, D. D. Solnyshkov, and G. Malpuech, Phys. Rev. B **82**, 153303 (2010).
[32] T. Espinosa-Ortega and T. C. H. Liew, Phys. Rev. B **87**, 195305 (2013).
[33] H. Flayac and I. G. Savenko, Appl. Phys. Lett. **103**, 201105 (2013).
[34] T. C. H. Liew, I. A. Shelykh, and G. Malpuech, Physica (Amsterdam) **43E**, 1543 (2011).
[35] C. Sturm *et al.*, arXiv:1303.1649 [Nat. Commun. (to be published)].
[36] K. G. Lagoudakis, M. Wouters, M. Richard, A. Baas, I. Carusotto, R. André, L. S. Dang, and B. Deveaud-Plédran, Nat. Phys. **4**, 706 (2008).
[37] K. G. Lagoudakis, T. Ostatnicky, A. V. Kavokin, Y. G. Rubo, R. Andre, and B. Deveaud-Pledran, Science **326**, 974 (2009).
[38] A. Amo *et al.*, Science **332**, 1167 (2011).
[39] R. Hivet *et al.*, Nat. Phys. **8**, 724 (2012).
[40] D. D. Solnyshkov, H. Flayac, and G. Malpuech, Phys. Rev. B **85**, 073105 (2012).
[41] D. D. Solnyshkov, H. Flayac, and G. Malpuech, Phys. Rev. B **85**, 073105 (2012).
[42] H. Flayac, D. D. Solnyshkov, and G. Malpuech, New J. Phys. **14**, 085018 (2012).
[43] H. Teras, D. Solnyshkov, and G. Malpuech, arXiv:1310.6588.
[44] I. A. Shelykh, A. V Kavokin, Y. G. Rubo, T. C. H. Liew, and G. Malpuech, Semicond. Sci. Technol. **25**, 013001 (2010).
[45] E. Wertz *et al.*, Nat. Phys. **6**, 860 (2010).
[46] H. Flayac, G. Pavlovic, M. A. Kaliteevski, and I. A. Shelykh, Phys. Rev. B **85**, 075312 (2012).
[47] M. Wouters and I. Carusotto, Phys. Rev. Lett. **99**, 140402 (2007).
[48] C. Antón, T. C. H. Liew, G. Tosi, M. D. Martín, T. Gao, Z. Hatzopoulos, P. S. Eldridge, P. G. Savvidis, and L. Viña, Phys. Rev. B **88**, 035313 (2013).
[49] I. G. Savenko, T. C. H. Liew, and I. A. Shelykh, Phys. Rev. Lett. **110**, 127402 (2013).
[50] Y. V. Kartashov and A. M. Kamchatnov, Opt. Lett. **38**, 790 (2013).
[51] See Supplemental Material at http://link.aps.org/supplemental/10.1103/PhysRevLett.112.140405 for a detailed analysis and numerics of the critical step size necessary to generate soliton trains.
[52] N. G. Berloff and P. H. Roberts, J. Phys. A **33**, 4025 (2000).
[53] M. Kaliteevski *et al.*, Phys. Rev. B **76**, 165415 (2007).
[54] C. W. Lai *et al.*, Nature (London) **450**, 529 (2007).
[55] T. C. H. Liew, A. V. Kavokin, T. Ostatnický, M. Kaliteevski, I. A. Shelykh, and R. A. Abram, Phys. Rev. B **82**, 033302 (2010).
[56] H. Flayac, H. Terças, D. D. Solnyshkov, and G. Malpuech, Phys. Rev. B **88**, 184503 (2013).
[57] N. Q. Ngo, Phot. Technol. Lett. **19**, 471 (2007).
[58] F. Pinsker, arXiv:1305.4088.
[59] E. Kammann, T. C. H. Liew, H. Ohadi, P. Cilibrizzi, P. Tsotsis, Z. Hatzopoulos, P. G. Savvidis, A. V. Kavokin, and P. G. Lagoudakis, Phys. Rev. Lett. **109**, 036404 (2012).